Classical and Quantum Liquids Induced by Quantum Fluctuations

Miguel M. Oliveira*
CeFEMA, Instituto Superior Técnico, Universidade de Lisboa avenida Rovisco Pais, 1049-001 Lisboa, Portugal

Pedro Ribeiro†
CeFEMA, Instituto Superior Técnico, Universidade de Lisboa avenida Rovisco Pais, 1049-001 Lisboa, Portugal and Beijing Computational Science Research Center, Beijing 100193, China

Stefan Kirchner‡
Zhejiang Institute of Modern Physics, Zhejiang University, Hangzhou, Zhejiang 310027, China and Zhejiang Province Key Laboratory of Quantum Technology and Devices, Zhejiang University, Hangzhou 310027, China

(Received 12 November 2018; revised manuscript received 16 March 2019; published 17 May 2019)

Geometrically frustrated interactions may render classical ground states macroscopically degenerate. The connection between classical and quantum liquids and how the degeneracy is affected by quantum fluctuations is, however, not completely understood. We study a simple model of coupled quantum and classical degrees of freedom, the so-called Falicov-Kimball model, on a triangular lattice and away from half-filling. For weak interactions the phase diagram features a charge disordered state down to zero temperature. We provide compelling evidence that this phase is a liquid and show that it is divided by a crossover line that terminates in a quantum critical point. Our results offer a new vantage point to address how quantum liquids can emerge from their classical counterparts.

DOI: 10.1103/PhysRevLett.122.197601

Liquids are characterized by the absence of long-range order. In exceptional cases, a classical liquid state may persist down to zero temperature [1,2]. The ensuing ground state is macroscopically degenerate and characterized by a finite entropy. Such a degeneracy in the energy landscape can result from competing interactions, geometric frustration, or near phase transitions where different states compete. The proliferation of low-energy states renders the system unstable towards the emergence of novel and often exotic ground states.

An interesting and still open issue concerns the relation between classical and quantum liquids, i.e., how quantum fluctuations affect the classical ground state manifold [3,4]. Another pertinent issue of practical relevance is the stability of such liquid phases with respect to, for example, the itinerary of the frustrated degrees of freedom (d.o.f.). Any attempt of answering these questions is faced with the principal difficulty that quantum fluctuations of competing interactions, covering a wide energy range, need to be taken into account.

In this Letter, we identify liquid phases that are driven by a coupling to quantum d.o.f. Depending on whether the quantum variables acquire a nonzero mass, the nature of the liquid phase changes. To this end, we study the Falicov-Kimball model (FKM), a hybrid model comprised of itinerant fermions that interact arbitrarily strongly with localized charges, on a triangular lattice. This model is well suited to address some of the unresolved issues mentioned above and, in addition, allows for an effective, numerically exact Monte Carlo sampling of its partition function [5,6].

The FKM can be thought of as a special case of the Hubbard model with infinite mass imbalance between the two spin species, thus rendering the dynamics of the heavier one classical. The position of these classical charges is annealed over an energy landscape defined by the itinerant d.o.f. The model has been instrumental in benchmarking the standard approach to strongly correlated lattice models, i.e., the dynamic mean field theory, and its extensions [7–12]. More recently, it has attracted interest in the context of disorder-free many-body localization [6,13,14]. For bipartite lattices, several exact results have been established [15,16], including the existence of a charge density wave (CDW) at low temperature (T) for all interaction strengths. The melting of the CDW state with increasing T was observed for commensurate fillings [15–18]. On the triangular lattice the FKM and its extensions display a variety of different ground-state phases [19–23]. For incommensurate fillings the FKM favors phase separation [5]. Recently, it was demonstrated that the half-filled model on the square lattice is nonmetallic at all nonvanishing values of the interaction strength U and transitions from Anderson to Mott insulators as U is varied [6].

An effective model for the classical charges can be derived perturbatively at sufficiently small coupling t/U, where t is the hopping strength of the itinerant electrons. At half-filling and for large U/t, the FKM is equivalent to the

antiferromagnetic Ising model. Thus, on the square lattice, order ensues at sufficiently low T whereas the large-U limit remains disordered for all T on the triangular lattice [1]. While it is an interesting question how this gets modified in the presence of quantum fluctuations [24], the parent state at large U is already a liquid. Here, however, we will in what follows demonstrate that a classical liquid state can result from an ordered phase, due to coupling to a quantum field.

The Hamiltonian of the FKM is

$$H = -t\sum_{\langle ij\rangle} c_i^\dagger c_j + U\sum_i c_i^\dagger c_i n_{f,i} - \mu_c \sum_i c_i^\dagger c_i - \mu_f \sum_i n_{f,i}, \tag{1}$$

where $c_i^\dagger$ creates a c electron and $n_{f,i}$, a conserved quantity, counts the number of immobile classical charges on site i, and μ is the chemical potential of the system. t will be used as a unit of energy ($t = 1$). The summation $\sum_{\langle i,j\rangle}$ runs over all nearest-neighbor pairs on a triangular lattice with a volume $V = L^2$ (L being the system's linear dimension) and periodic boundary conditions. As the collection of $n_{f,i}$ constitutes a set of conserved quantities, the partition function is given by a summation over noninteracting contributions for every configuration n_f of f charges and thus can be evaluated by an efficient Monte Carlo sampling [5,6]. An additional difficulty arises as the chemical potentials $\mu_c(T, U, L)$ and $\mu_f(T, U, L)$ need to be self-consistently determined to ensure constant occupation as a function of T, U, and L (Ref. [25], S2).

In the following, we consider a macrocanonical ensemble with the chemical potentials μ_c and μ_f determined such that $x_c = N_c/V = 2/3$ and $x_f = N_f/V = 1/3$, where $N_c = \langle \sum_i c_i^\dagger c_i \rangle$ and $N_f = \sum_i \langle n_{f,i} \rangle$, see, however, the Supplemental Material S6 [25]. Our findings are summarized in the phase diagram of Fig. 1. At large U and sufficiently low T, $[T < T_c(U)]$, the system develops a CDW. For large T and/or U, the phase diagram resembles that of its counterpart on the square lattice. While this could have been anticipated, there are important differences with regard to the type of order, see below. The most surprising feature is the two regions at low T and small U, labeled classical charge liquid (CL) and quantum charge liquid (QL), respectively, that remain disordered down to the lowest T. At large U, the T-driven phase transition is continuous and within the universality class of the three-state Potts model. For small U, our data point to a discontinuous transition between the CDW and the CL down to $T_c(U_c) = 0$, corresponding to $U_c \simeq 5.2$. For large T, a "strange metal region" (WL) is found, where the electrons are weakly localized, followed by an Anderson insulating (AI) and finally a Mott insulting (MI) phase as U increases which arises due to the condition $x_c + x_f = 1$, generalizing the half-filling condition of the (spinfull) Hubbard model. The WL region is only stabilized by

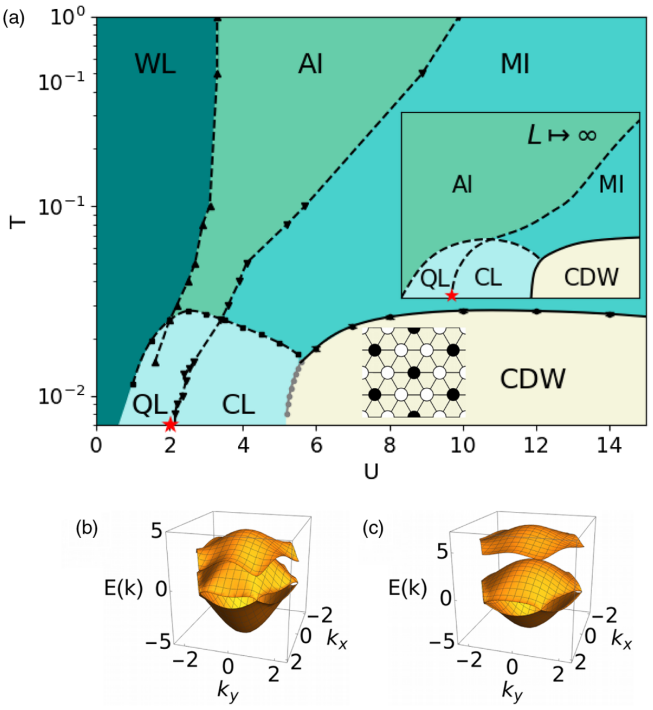

FIG. 1. (a) Phase diagram of the FK model on the triangular lattice in the T-U plane for $x_f = 1/3$ and $x_c = 2/3$. The red star indicates the quantum phase transition between the liquid states. The inset depicts a sketch of the phases in the thermodynamic limit. Band structure assuming CDW order for $U = 2$ (b) and $U = 5$ (c).

the finite extent of the system and is expected to vanish in the thermodynamic limit [6]. AI is characterized by a finite density of states (DOS) at the Fermi level and a volume-independent inverse participation ratio (IPR). In the MI phase, the chemical potential lies within a U-dependent spectral gap. This all closely resembles earlier findings for the FKM on a square lattice of Ref. [6], where a full characterization of these phases, including a discussion of the optical conductivity, can be found. In what follows, we focus on the fundamentally new features that emerge from the interplay of localized and itinerant d.o.f. in a geometrically frustrated environment.

In the expansion in terms of t/U, higher order terms beyond the nearest-neighbor Ising-like interaction proportional to t^2/U can be systematically derived [26]. In next-to-leading order, i.e., t^3/U^2, it yields a term that couples the d.o.f. on a triangular plaquette. The range of the effective interaction increases with powers of t/U, increasing the frustration that eventually leads to the melting of the order. This procedure is carried out in Ref. [25] up to order t^4/U^3.

At large U, the effective term together with the $x_f = 1/3$ restriction favors the existence of a low-T ordered phase possessing a threefold degeneracy. A possible order parameter for this phase is $\phi_{1/3} = (3/V)\sum_r e^{i(2\pi/3)(r_x - r_y)} n_{f,r}$ that equals $\phi_{1/3} = 1, e^{i(2\pi/3)}$ or $e^{i(4\pi/3)}$ depending on which of the three degenerate ground states is realized. One such

configuration is depicted in the inset of Fig. 1, while the others can be obtained by a translation.

The order parameter symmetry implies that the associated finite-T transition belongs to the two-dimensional three-state Potts model universality class. We find for the correlation length exponent $\nu = 0.8031(114)$ (cf. $\nu_{3\mathrm{Potts}} = 5/6$ [31]) and for γ, the exponent of the T dependence of the susceptibility of the f charges, $\gamma = 1.4748(329)$ (cf. $\gamma_{3\mathrm{Potts}} = 13/9$ [31]); for details, see the Supplemental Material [25].

The specific heat C_v across the charge ordering transition for $U = 7$ is shown in Fig. 2(c). A high-T local maximum (not shown in the figure) coincides with the T scale where double occupancy is sharply suppressed as T is lowered. At lower T, the divergent C_v, confirmed by the finite-size scaling, corresponds to the transition into the CDW state. The static susceptibility, $\chi(\omega \to 0, q, T)$ is depicted in Fig. 2(f). It shows a maximum at the propagation vector Q_{CDW} of the CDW, i.e., $q = Q_{\mathrm{CDW}} = 2\pi/3\{1, \sqrt{3}\}$. Figure 2(e) (orange line) shows that, for $T < T_c$, $\chi(\omega \to 0, \mathbf{Q}_{\mathrm{CDW}}, T) \propto L^2$, in line with the existence of long-range order. The reconstructed band structure of the c electrons within this symmetry broken phase at $T = 0$ is given in Fig. 1(c); μ_c lies in the U-dependent band gap. Assuming that the ordered phase persists as a function of U one expects an indirect closing of the band gap for $U = 3$. Figure 1(b) shows the band structure for $U < 3$. The charge order, however, vanishes at $U_c > 3$; see Fig. 1(a).

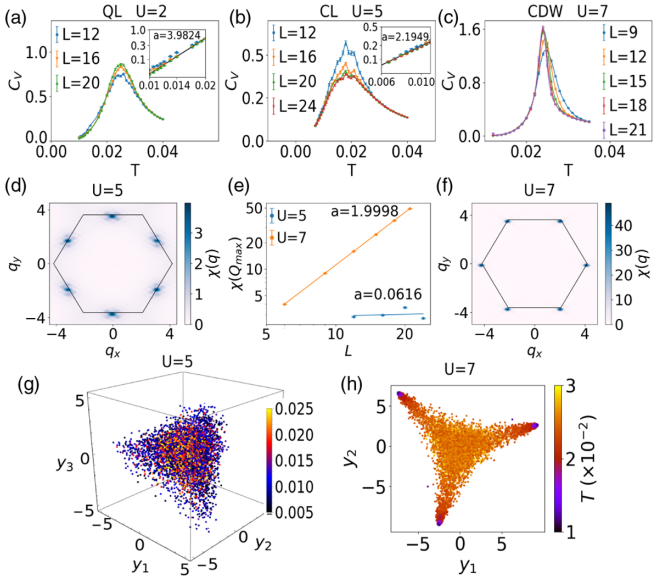

FIG. 2. Specific heat as a function of T for $U = 2$ (a), $U = 5$ (b), and $U = 7$ (c). Momentum resolved susceptibility of the f charges $\chi(q)$ for $U = 5$ (d) and $U = 7$ (f). (e) Finite size scaling of $\chi(Q_{\mathrm{Max}})$ with L. PCA yielding (g) the 3 most important components for $U = 5$ and (h) 2 for $U = 7$, plotted for a range of T for $L = 20$ and $L = 21$, respectively, see Supplemental Material (s4)[25].

We now address the region $U < U_c$. Figures 2(a) and 2(b) show $C_v(T)$ in this region for a representative value of U within the QL and CL, respectively. The high-T features are similar to those found for $U > U_c$. In contrast to the $U > U_c$ case, $C_v(T, L)$ remains nonsingular for $L \to \infty$, indicating that the transition has been replaced by a crossover. The insets of Figs. 2(a) and 2(b) depict $C_v(T)$ on a logarithmic scale and indicate that the behavior is compatible with power-law scaling in T implying gapless excitations in the system. The fact that both power laws are distinct highlights that there are indeed two different $T = 0$ phases. Moreover, neither is compatible with Fermi-liquid behavior, i.e., with $C_v(T) \propto T$. Within these phases, $\chi(0, \boldsymbol{q}, T)$ is no longer maximal for $\boldsymbol{q} = \boldsymbol{Q}_{\mathrm{CDW}}$ but rather for $\boldsymbol{q} = \boldsymbol{Q}_{\mathrm{Max}} = \pi\{1, 1/\sqrt{3}\}$, as shown in Fig. 2(d) for CL (similar for QL). Interestingly, $\boldsymbol{Q}_{\mathrm{Max}}$ corresponds to the wave vector of a CDW expected for filling fractions $x_f = 1/4$ and $x_c = 3/4$; see Fig. 2(d). However, the order parameter $\phi_{1/4}$ of this phase, explicitly given in Ref. [25], vanishes (see below). The scaling of $\chi(0, \boldsymbol{Q}_{\mathrm{Max}}, T)$ with L shown in Fig. 2(e) (blue line) is $\chi(\omega \to 0, \boldsymbol{Q}_{\mathrm{Max}}, T) \propto L^a$ with $a \simeq 0.0616$, which indicates that the CL region is incompatible with the existence of long-range order of that type. To further substantiate the characterization of the liquid region, we turn to a principal component analysis (PCA) [32] of the charge excitations in CL and CDW. This method allows for a dimensional reduction when visualizing multivariate data [27]. Figures 2(g) and 2(h) show the projection of different thermalized configurations onto the three principal components obtained by a PCA analysis including uncorrelated configurations at different T, see the Supplemental Material (S4) [25]. In the ordered phase, low-T configurations cluster around one of the three ground states; see Fig. 2(h), which correspond to two principal components. Within the CL region, however, configurations cluster on a fourfold symmetric structure corresponding to three principal components. Note, however, that this does not imply the existence of a long-range ordered fourfold state, which is incompatible with the $1/3$ filling, unless phase separation occurs. A vanishing order parameter and associated susceptibility $\chi(0, \boldsymbol{Q}_{\mathrm{Max}}, T) = \chi(L)$ as $L \to \infty$ is, however, incompatible with phase separation, see Fig. 2(e) [25].

Another possibility in line with the power-law behavior in $\chi(L)$ and $C_v(T)$ for $T \to 0$ is the occurrence of a phase transition, at a T near the low-T peak in the specific heat, to a KT-like phase, lacking long-range order. Indeed, KT transitions can occur for clock models with Z_q symmetry [33]. While our numerical results alone cannot exclude this scenario, this only arises for clock models with $q > 4$ [33–35]. Moreover the system seems to retain its full symmetry, isomorphic to the permutation group and not just a Z_4 subgroup.

The only viable alternative for the low T, low U regions of the phase diagram is the existence of charge liquid states,

connected by a smooth crossover to the charge-disordered state at high T. The observed behavior in C_v vs L is indeed in line with such a crossover, see Figs. 2(a) and 2(b) as is its $T \to 0$ behavior, as discussed above.

In order to understand the difference between CL and QL we study the properties of the c electrons through their DOS and IPR. Figure 1 shows the liquid region is intersected by the AI-MI crossover line defined by the vanishing of the DOS at zero energy. At $T = 0$, this crossover line should terminate in a continuous Mott transition separating two phases where the c electrons pass from being gapless to being gapped as U increases. Figures 3(a) and 3(c) show the DOS as a function of energy for two values of U; one below (a) and the other (c) for U above the AI-MI crossover line separating the QL and CL regions. Figure 3(c) shows that in the MI side there is a region around $\omega = 0$ without c-electron states in contrast to the finite DOS around $\omega = 0$ seen in Fig. 3(a). The inset of Fig. 3(c) depicts the behavior of the DOS$(\omega = 0)$ vs U for different T showing a sharp drop. This sharp drop is used to determine the crossover line.

Figure 3(b) shows an example of the IPR(ω) in the vicinity of the Fermi energy and its scaling with system size for a case where IPR$(\omega = 0)$ converges to a finite value as a function of L. Figure 3(d) depicts the scaling of IPR$(\omega = 0)$ as a function of system size. The crossover line separating the WL from the AI region signals the localization-delocalization transition of the c electrons and is obtained from the scaling behavior of IPR$(\omega = 0)$ with volume. This IPR$(\omega = 0)$ line can be continued into the QL region; see Fig. 1.

The WL is expected to vanish as the thermodynamic limit is taken [6]. However, there is the interesting possibility that the fate of the delocalized region as the thermodynamic limit is taken, is different from that of WL, as the sampled disorder configurations in the CL region are highly correlated. This would allow for an itinerant c electron phase in the thermodynamic limit. Our data, however, do not permit us to discriminate between these scenarios due to dominating finite-size effects.

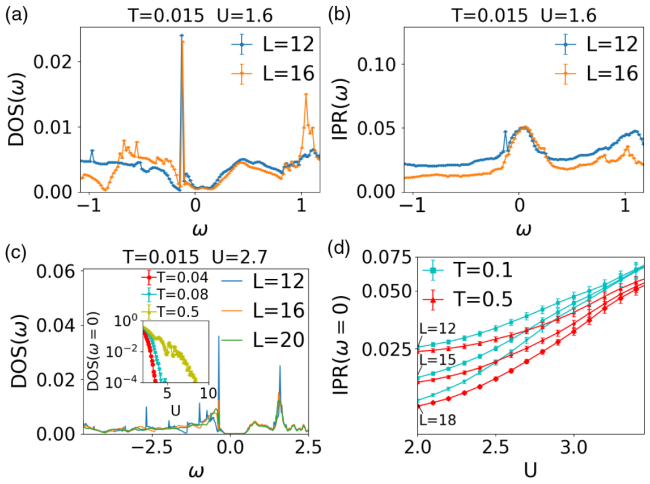

FIG. 3. c-electron properties: DOS for $U = 1.6$ (a) and $U = 2.7$ (c) for $T = 0.015$. Inset of (c) shows DOS$(\omega = 0)$ vs U for different T. IPR as a function of energy for different system sizes (b). (d) Scaling of the IPR$(\omega = 0)$ as a function of U. Data obtained from simulations with 100 000 Monte Carlo steps with correlation times of at most 20 steps.

Figure 4(a) shows the order parameters of $\phi_{1/3}$ and $\phi_{1/4}$ of the (full) FK model. The inset shows that the amplitude of $\phi_{1/4}$ vanishes in the thermodynamic limit as L^a with $a \simeq -1$.

Within our numerical precision, the nature of the CL-CDW transition in Fig. 4(a) is compatible with a discontinuous transition with double-peaked distribution of the order parameter and energy. The Binder cumulant, however, remains positive near the transition (see the Supplemental Material [25]). In order to avoid spurious finite-size effects we only consider $L = 12$, 24, which are commensurate with both the CDW and the incipient 1/4-filling ordered background.

To further analyze the origin of the CL phase we turn to a study of the effective classical model, see the Supplemental Material [25], using a Monte Carlo algorithm. Figure 4(b) depicts the same quantities but for the effective classical model obtained by truncating the expansion to fourth order and where the effective couplings are replaced by their $T = 0$ limits. The inset of 4(b) schematically depicts the different coupling terms of the effective Hamiltonian. In contrast with the FK model the truncated one exhibits a phase separated state at small U characterized by a nonvanishing value of $\phi_{1/4}$. Figure 4(c) shows $\phi_{1/3}$ and $\phi_{1/4}$ for an effective model with the same type of interactions as 4(b) but with the coupling constants determined by linear regressions [28], explicitly given in Ref. [25]. The inset demonstrates that $\phi_{1/4}$ indeed vanishes albeit with a different power of the linear system size $a \sim -1/2$.

In the QL, the gapless quantum d.o.f. induce long-ranged interactions among the classical charges. In contrast, for the CL, we expect that an effective Hamiltonian exists in terms of short-ranged classical charges. Up to fourth order, however, neither the truncated model nor the variational

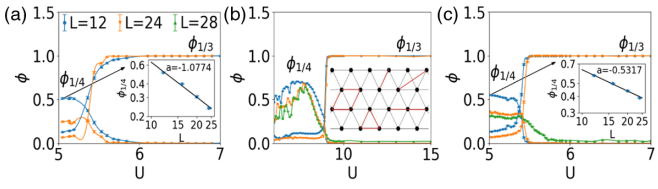

FIG. 4. Order parameters $\phi_{1/3}$ and $\phi_{1/4}$ for (a) the FK model, (b) the effective classical model truncated to 4th order, (c) an effective variational model, with couplings determined by a linear regression. The inset of (a) and (c) show the scaling of the $\phi_{1/4}$ with system sizes for $U = 5$, respectively, for the FK and variational models. The inset in (b) depicts the schematic couplings between sites obtained up to 4th order.

one seem to capture the properties of the CL phase. Apparently, higher order terms are necessary to fully capture the properties of this phase. We thus have obtained an unexpectedly rich phase diagram of the 1/3-filled FKM on the triangular lattice: for intermediate-to-large coupling, the T-driven phase transition from the charge-ordered to the disordered phase belongs to the three-state Potts model universality class; more importantly, for weak coupling and low T, we show the existence of a charge liquid region divided by a crossover line that terminates in a QCP at U_{QCP}. The classical liquid, which ensues for $U > U_{\mathrm{QCP}}$, is expected to be captured by an effective, finite-ranged classical model. However, we were not able to obtain such a model with terms up to the fourth order in terms of t/U. Approaching the QCP from within the CL, the gap of the quantum d.o.f. vanishes at U_{QCP}. This phase transition is reflected in the behavior of the specific heat which changes from $C_v \propto T^2$ to $C_v \propto T^4$ as U_{QCP} is crossed. To better understand the differences between the full and the truncated classical model it will be instructive to analyze the effect of higher orders systematically [36].

Our results show how quantum liquids can emerge from their classical counterparts. They also elucidate how classical liquids form through melting of phase separated states in the presence of frustrated interactions. Addressing the fate of the charge liquids in the presence of nonvanishing hybridization between the localized charges and the conduction electrons is an interesting open question with immediate experimental relevance [37,38]. Understanding the fate of the CL phase as the FKM approaches the Hubbard model may help unraveling the phase diagram of the Hubbard model on the triangular lattice [39].

We gratefully acknowledge helpful discussions with A. Antipov, R. Mondaini, A. Sandvik, and D. Vollhardt. Computations were performed on the Tianhe-2JK cluster at the Beijing Computational Science Research Center (CSRC) and on the Baltasar-Sete-Sóis cluster, supported by V. Cardoso's H2020 ERC Consolidator Grant No. MaGRaTh-646597, computer assistance was provided by CSRC and CENTRA/IST. M. M. O. acknowledges partial support by the FCT through IF/00347/2014/CP1214/CT0002 and SFRH/BD/137446/2018. P. R. acknowledges support by FCT through the Investigador FCT Contract No. IF/00347/2014 and Grant No. UID/CTM/04540/2013. S. K. acknowledges support by the National Science Foundation of China, Grants No. 11474250 and No. 11774307 and the National Key R&D Program of the MOST of China, Grant No. 2016YFA0300202.

*miguel.m.oliveira@tecnico.ulisboa.pt
†ribeiro.pedro@gmail.com
‡stefan.kirchner@correlated-matter.com

[1] G. H. Wannier, Phys. Rev. **79**, 357 (1950).
[2] C. Castelnovo, R. Moessner, and S. L. Sondhi, Nature (London) **451**, 42 (2008).
[3] I. Rousochatzakis, Y. Sizyuk, and N. B. Perkins, Nat. Commun. **9**, 1575 (2018).
[4] Y. Zhou, K. Kanoda, and T.-K. Ng, Rev. Mod. Phys. **89**, 025003 (2017).
[5] M. M. Maśka and K. Czajka, Phys. Status Solidi (b) **242**, 479 (2005).
[6] A. E. Antipov, Y. Javanmard, P. Ribeiro, and S. Kirchner, Phys. Rev. Lett. **117**, 146601 (2016).
[7] W. Metzner and D. Vollhardt, Phys. Rev. Lett. **62**, 324 (1989).
[8] A. Georges, G. Kotliar, W. Krauth, and M. J. Rozenberg, Rev. Mod. Phys. **68**, 13 (1996).
[9] U. Brandt and C. Mielsch, Z. Phys. B **75**, 365 (1989).
[10] J. Freericks and V. Zlatić, Rev. Mod. Phys. **75**, 1333 (2003).
[11] A. E. Antipov, E. Gull, and S. Kirchner, Phys. Rev. Lett. **112**, 226401 (2014).
[12] G. Rohringer, H. Hafermann, A. Toschi, A. A. Katanin, A. E. Antipov, M. I. Katsnelson, A. I. Lichtenstein, A. N. Rubtsov, and K. Held, Rev. Mod. Phys. **90**, 025003 (2018).
[13] A. Smith, J. Knolle, D. L. Kovrizhin, and R. Moessner, Phys. Rev. Lett. **118**, 266601 (2017).
[14] A. Smith, J. Knolle, R. Moessner, and D. L. Kovrizhin, Phys. Rev. Lett. **119**, 176601 (2017).
[15] U. Brandt and R. Schmidt, Z. Phys. B **63**, 45 (1986).
[16] T. Kennedy and E. H. Lieb, Physica (Amsterdam) **138A**, 320 (1986).
[17] M. M. Maśka and K. Czajka, Phys. Rev. B **74**, 035109 (2006).
[18] M. Žonda, P. Farkašovský, and H. Čenčariková, Solid State Commun. **149**, 1997 (2009).
[19] H. Čenčariková and P. Farkašovský, Phys. Status Solidi (b) **244**, 1900 (2007).
[20] U. K. Yadav, T. Maitra, I. Singh, and A. Taraphder, J. Phys. Condens. Matter **22**, 295602 (2010).
[21] U. K. Yadav, T. Maitra, and I. Singh, Eur. Phys. J. B **84**, 365 (2011).
[22] U. K. Yadav, T. Maitra, I. Singh, and A. Taraphder, Europhys. Lett. **93**, 47013 (2011).
[23] S. Kumar, U. K. Yadav, T. Maitra, and I. Singh, AIP Conf. Proc. **1731**, 030014 (2016).
[24] M. M. Oliveira *et al.*, The half-filled Falicov-Kimball model on the triangular lattice: classical to quantum charge liquid (to be published).
[25] See Supplemental Material at http://link.aps.org/supplemental/10.1103/PhysRevLett.122.197601 for additional technical details and further numerical results supplementing the conclusions from the main text, which includes Refs. [26–30].
[26] C. Gruber, N. Macris, A. Messager, and D. Ueltschi, J. Stat. Phys. **86**, 57 (1997).
[27] L. Wang, Phys. Rev. B **94**, 195105 (2016).
[28] J. Liu, Y. Qi, Z. Y. Meng, and L. Fu, Phys. Rev. B **95**, 041101(R) (2017).
[29] Z. Wang, F. F. Assaad, and F. Parisen Toldin, Phys. Rev. E **96**, 042131 (2017).
[30] H. Fehske, R. Schneider, and A. Weiße, *Computational Many-Particle Physics*, Lecture Notes in Physics (Springer, Berlin Heidelberg, 2010), Chap. 4.

[31] R. J. Baxter, *Exactly Solved Models in Statistical Mechanics* (Academic Press Limited, Cambridge, 1982).
[32] J. Ian, Principal component analysis, in *Wiley StatsRef: Statistics Reference Online* (American Cancer Society, Hoboken, 2014).
[33] S. Elitzur, R. B. Pearson, and J. Shigemitsu, Phys. Rev. D **19**, 3698 (1979).
[34] P. Ruján, G. O. Williams, H. L. Frisch, and G. Forgács, Phys. Rev. B **23**, 1362 (1981).
[35] S. K. Baek and P. Minnhagen, Phys. Rev. E **82**, 031102 (2010).
[36] H.-Y. Yang, A. F. Albuquerque, S. Capponi, A. M. Läuchli, and K. P. Schmidt, New J. Phys. **14**, 115027 (2012).
[37] S. Nakatsuji, Y. Machida, Y. Maeno, T. Tayama, T. Sakakibara, J. van Duijn, L. Balicas, J. N. Millican, R. T. Macaluso, and J. Y. Chan, Phys. Rev. Lett. **96**, 087204 (2006).
[38] Y. Tokiwa, J. J. Ishikawa, S. Nakatsuji, and P. Gegenwart, Nat. Mater. **13**, 356 (2014).
[39] G. Li, A. E. Antipov, A. N. Rubtsov, S. Kirchner, and W. Hanke, Phys. Rev. B **89**, 161118(R) (2014).